

World Journal of *Gastrointestinal Oncology*

World J Gastrointest Oncol 2021 August 15; 13(8): 758-979



REVIEW

- 758 Metabolism-associated genes in occurrence and development of gastrointestinal cancer: Latest progress and future prospect
Miao YD, Mu LJ, Mi DH
- 772 Immune checkpoint inhibitor-mediated colitis in gastrointestinal malignancies and inflammatory bowel disease
Weingarden AR, Rubin SJS, Gubatan J
- 799 B7 homologue 3 as a prognostic biomarker and potential therapeutic target in gastrointestinal tumors
Rasic P, Jovanovic-Tucovic M, Jeremic M, Djuricic SM, Vasiljevic ZV, Milickovic M, Savic D

MINIREVIEWS

- 822 Reflectance spectra analysis for mucous assessment
Chiba T, Murata M, Kawano T, Hashizume M, Akahoshi T
- 835 *Helicobacter pylori* infection and other bacteria in pancreatic cancer and autoimmune pancreatitis
Kunovsky L, Dite P, Jabandzic P, Dolina J, Vaculova J, Blaho M, Bojkova M, Dvorackova J, Uvirova M, Kala Z, Trna J
- 845 Recent update on comprehensive therapy for advanced hepatocellular carcinoma
Wang H, Li W
- 856 Young-onset colorectal cancer: A review
Done JZ, Fang SH
- 867 Role of exosomal long non-coding RNAs in colorectal cancer
Sun R, He XY, Mei C, Ou CL

ORIGINAL ARTICLE**Basic Study**

- 879 Plasma MMP-2 and MMP-7 levels are elevated first month after surgery and may promote growth of residual metastases
Shantha Kumara H, Miyagaki H, Herath SA, Pettke E, Yan X, Cekic V, Whelan RL
- 893 STAT3-mediated activation of mitochondrial pathway contributes to antitumor effect of dihydrotanshinone I in esophageal squamous cell carcinoma cells
Qi MM, He PZ, Zhang L, Dong WG

Retrospective Cohort Study

- 915** Neutrophil-to-lymphocyte ratio and carbohydrate antigen 19-9 as prognostic markers for advanced pancreatic cancer patients receiving first-line chemotherapy

Shin K, Jung EK, Park SJ, Jeong S, Kim IH, Lee MA

Retrospective Study

- 929** Diffuse reduction of spleen density is a novel prognostic marker for intrahepatic cholangiocarcinoma after curative resection

Deng LM, Wang Y, Yang JH, Li JL, Chen ZY, Bao WM, Chen KY, Yao XF, Zheng CM, Zheng JY, Yu ZP, Jin B, Chen G

- 943** Development of a prognostic prediction model based on microRNA-1269a in esophageal cancer

Yu Y, Ren KM

- 959** Investigation of the factors influencing surgical treatment of duodenal gastrointestinal stromal tumors

Wu YZ, Li Y, Wu M, Zheng XH, Tian YT, Xie YB

Observational Study

- 970** Diagnostic value of four serum exosome microRNAs panel for the detection of colorectal cancer

Han L, Shi WJ, Xie YB, Zhang ZG

ABOUT COVER

Editorial Board Member of *World Journal of Gastrointestinal Oncology*, Renato Borges Fagundes, MD, PhD, Full Professor, Gastroenterology Department of Hospital Universitário de Santa Maria, Universidade Federal de Santa Maria, Porto Alegre 90480200, Brazil. fagundesrb@gmail.com

AIMS AND SCOPE

The primary aim of *World Journal of Gastrointestinal Oncology* (*WJGO*, *World J Gastrointest Oncol*) is to provide scholars and readers from various fields of gastrointestinal oncology with a platform to publish high-quality basic and clinical research articles and communicate their research findings online.

WJGO mainly publishes articles reporting research results and findings obtained in the field of gastrointestinal oncology and covering a wide range of topics including liver cell adenoma, gastric neoplasms, appendiceal neoplasms, biliary tract neoplasms, hepatocellular carcinoma, pancreatic carcinoma, cecal neoplasms, colonic neoplasms, colorectal neoplasms, duodenal neoplasms, esophageal neoplasms, gallbladder neoplasms, etc.

INDEXING/ABSTRACTING

The *WJGO* is now indexed in Science Citation Index Expanded (also known as SciSearch®), PubMed, PubMed Central, and Scopus. The 2021 edition of Journal Citation Reports® cites the 2020 impact factor (IF) for *WJGO* as 3.393; IF without journal self cites: 3.333; 5-year IF: 3.519; Journal Citation Indicator: 0.5; Ranking: 163 among 242 journals in oncology; Quartile category: Q3; Ranking: 60 among 92 journals in gastroenterology and hepatology; and Quartile category: Q3. The *WJGO*'s CiteScore for 2020 is 3.3 and Scopus CiteScore rank 2020: Gastroenterology is 70/136.

RESPONSIBLE EDITORS FOR THIS ISSUE

Production Editor: *Ying-Yi Yuan*; Production Department Director: *Xiang Li*; Editorial Office Director: *Ya-Juan Ma*.

NAME OF JOURNAL

World Journal of Gastrointestinal Oncology

ISSN

ISSN 1948-5204 (online)

LAUNCH DATE

February 15, 2009

FREQUENCY

Monthly

EDITORS-IN-CHIEF

Rosa M Jimenez Rodriguez, Pashtoon Kasi, Monjur Ahmed, Florin Burada

EDITORIAL BOARD MEMBERS

<https://www.wjgnet.com/1948-5204/editorialboard.htm>

PUBLICATION DATE

August 15, 2021

COPYRIGHT

© 2021 Baishideng Publishing Group Inc

INSTRUCTIONS TO AUTHORS

<https://www.wjgnet.com/bpg/gerinfo/204>

GUIDELINES FOR ETHICS DOCUMENTS

<https://www.wjgnet.com/bpg/GerInfo/287>

GUIDELINES FOR NON-NATIVE SPEAKERS OF ENGLISH

<https://www.wjgnet.com/bpg/gerinfo/240>

PUBLICATION ETHICS

<https://www.wjgnet.com/bpg/GerInfo/288>

PUBLICATION MISCONDUCT

<https://www.wjgnet.com/bpg/gerinfo/208>

ARTICLE PROCESSING CHARGE

<https://www.wjgnet.com/bpg/gerinfo/242>

STEPS FOR SUBMITTING MANUSCRIPTS

<https://www.wjgnet.com/bpg/GerInfo/239>

ONLINE SUBMISSION

<https://www.f6publishing.com>

Reflectance spectra analysis for mucous assessment

Toru Chiba, Masaharu Murata, Takahito Kawano, Makoto Hashizume, Tomohiko Akahoshi

ORCID number: Toru Chiba 0000-0001-5564-8929; Masaharu Murata 0000-0002-5625-2245; Takahito Kawano 0000-0002-6315-4117; Makoto Hashizume 0000-0002-5140-0982; Tomohiko Akahoshi 0000-0002-1750-2299.

Author contributions: Chiba T, Murata M, Akahoshi T, and Hashizume M conceived the paper; Murata M and Chiba T designed and co-ordinated the writing; Chiba T performed statistical analysis.

Conflict-of-interest statement: Authors declare no conflict of interests for this article.

Open-Access: This article is an open-access article that was selected by an in-house editor and fully peer-reviewed by external reviewers. It is distributed in accordance with the Creative Commons Attribution NonCommercial (CC BY-NC 4.0) license, which permits others to distribute, remix, adapt, build upon this work non-commercially, and license their derivative works on different terms, provided the original work is properly cited and the use is non-commercial. See: <http://creativecommons.org/licenses/by-nc/4.0/>

Manuscript source: Invited manuscript

Specialty type: Oncology

Toru Chiba, Pentax_LifeCare, HOYA Corporation, Akishima-shi 196-0012, Tokyo, Japan

Masaharu Murata, Takahito Kawano, Makoto Hashizume, Center for Advanced Medical Innovation, Kyushu University, Fukuoka-shi 812-8582, Fukuoka, Japan

Tomohiko Akahoshi, Department of Disaster and Emergency Medicine, Graduate School of Medical Sciences, Kyushu University, Fukuoka_shi 812-8582, Fukuoka, Japan

Corresponding author: Toru Chiba, BSc, Associate Specialist, Pentax_LifeCare, HOYA Corporation, Pentax Life Care Division Showanomori Technology Center 1-1-110 Tsutsujigaoka, Akishima-shi 196-0012, Tokyo, Japan. toru.chiba@pentaxmedical.com

Abstract

This review report represents an overview of research and development on medical hyperspectral imaging technology and its applications. Spectral imaging technology is attracting attention as a new imaging modality for medical applications, especially in disease diagnosis and image-guided surgery. Considering the recent advances in imaging, this technology provides an opportunity for two-dimensional mapping of oxygen saturation (SatO₂) of blood with high accuracy, spatial spectral imaging, and its analysis and provides detection and diagnostic information about the tissue physiology and morphology. Multispectral imaging also provides information about tissue oxygenation, perfusion, and potential function during surgery. Analytical algorithm has been examined, and indication of accurate map of relative hemoglobin concentration and SatO₂ can be indicated with preferable resolution and frame rate. This technology is expected to provide promising biomedical information in practical use. Several studies suggested that blood flow and SatO₂ are associated with gastrointestinal disorders, particularly malignant tumor conditions. The use and analysis of spectroscopic images are expected to potentially play a role in the detection and diagnosis of these diseases.

Key Words: Diffuse reflectance spectroscopy; Endoscopy; Hemoglobin saturation; Hypoxia; Gastrointestinal cancer; Tumor

©The Author(s) 2021. Published by Baishideng Publishing Group Inc. All rights reserved.

Core Tip: Hemoglobin saturation relative hemoglobin concentration diffuse reflectance spectroscopic. The use of spectroscopic information for pathological diagnosis and

Country/Territory of origin: Japan**Peer-review report's scientific quality classification**Grade A (Excellent): 0
Grade B (Very good): B
Grade C (Good): 0
Grade D (Fair): 0
Grade E (Poor): 0**Received:** March 1, 2021**Peer-review started:** March 1, 2021**First decision:** April 19, 2021**Revised:** April 26, 2021**Accepted:** July 9, 2021**Article in press:** July 9, 2021**Published online:** August 15, 2021**P-Reviewer:** Teramoto-Matsubara OT**S-Editor:** Fan JR**L-Editor:** A**P-Editor:** Ma YJ

detection has been studied. Detailed analysis of this information will contribute to the development of novel objective diagnostic techniques for diseases. In the latest research, it has become possible to visualize pathological conditions by indicating the two-dimensional distribution of blood concentration and oxygen saturation in real time, which can be realized without dosage. In the near future, derived research field that can be greatly expected to develop into future prediction of pathological conditions when performed in combination with statistical methods.

Citation: Chiba T, Murata M, Kawano T, Hashizume M, Akahoshi T. Reflectance spectra analysis for mucous assessment. *World J Gastrointest Oncol* 2021; 13(8): 822-834**URL:** <https://www.wjgnet.com/1948-5204/full/v13/i8/822.htm>**DOI:** <https://dx.doi.org/10.4251/wjgo.v13.i8.822>

INTRODUCTION

Studies on spectral characterization for visible using the diffuse reflectance method have been reported for various diseases. In recent years, the diffuse reflectance method has been applied to measure changes in perfusion in response to operations, such as infusion of vasoactive agents and cardiopulmonary bypass, and is expected to be applied to various fields, such as emergency medical monitoring of condition of blood flow and activity of the tissue[1,2]. Spectral characterization of tissue in the intestinal tract by combining the diffuse reflection method and the endoscope was reported[3].

For the past 20 years, spectral data capture technology using the diffuse reflectance method has been used in actual clinical trials, and its technique has expanded from spectral measurement using single or several fibers to multispectral imaging method, which focuses on the characteristic changes of the target.

In this report, measuring methods and analyses to date based on visible light spectra and its developments of several devices from the early stage to the present day are focused. There are two main types of spectral information: Hyperspectral data and multispectral data. In general, a series of information collected at a consecutive wavelength with 1-5 nm interval in defined wavelength area is treated as hyperspectral data, and information collected at some specific and discrete wavelength area is treated as multispectral data, which focuses on characteristic spectral information. Both appear to be positioned as part of diffuse reflectance spectroscopy, but there are major differences in the functions required of the equipment depending on the purpose. All information in the target wavelength region is required to elucidate the information of unknown substances. Collecting hyperspectral information always requires complicated equipment as well as a long capturing and analysis time, which prevents its practical use.

By contrast, in the case of tracking change for committed spectral information, it may be possible to collect information in a limited wavelength range with a higher data rate. For the development of practical equipment, which is using multispectral information, the aggregation of hyperspectral information is necessary.

The development of devices for the actual clinical field is actively promoted[4]. Results of the current applied research indicated the possibility that diffuse reflectance and multispectral technological methods will evolve into devices that may be useful in actual clinical practice in the near future[5-7]. Several studies reported on the use of spectroscopic information for gastrointestinal disorders. Some studies have used spectroscopic information peculiar to diseases and reports based on hemodynamics; however, the latter is a report focusing on high blood flow and hypoxia in malignant tumors. Supporting information for disease detection and diagnosis based on this information will make a great contribution to the field of diagnostic imaging.

With the advancement of equipment development, results obtained in this study are expected to be applied for practical use.

Based on the history of research and development of research and equipment, the report will cover the following contents: (1) Diffuse reflectance spectroscopy (DRS) and endoscope: Spectral information in the biomedical field; (2) Analysis of scattering information; (3) DRS data analysis; (4) Method of spectral image capturing: Hyper-spectral image capturing and equipment; (5) Practical use of multispectral analysis; and (6) Discussion: Application of reflectance spectroscopy, reflectance spectroscopy

as a future technology.

DRS AND ENDOSCOPE

In recent years, spectral observations through a fiber that has passed through a video endoscope and its accessory channel have been reported in a case, in which a spectral image of the large intestinal mucosa was captured using the combination of endoscope and spectral imaging device[8-18]. It has become possible to use objective information, including spectrochemical information, as well as the doctor's subjective diagnosis based on single image information. Other studies have reported that relative diffuse spectral information on the inner surface of the colon was dominated by relative hemoglobin concentration (r-Hconc), oxygen saturation (SatO₂), and scattering information[19-21].

Most of the hemoglobin in blood is in red blood cells in vessels, and the measured mucosal SatO₂ indicates tissue capillary oxygenation in both hypoxic and ischemic tissue. The SatO₂ of the mucosa is known to differ from the arterial SatO₂[22-24]. In addition, the relationship among blood flow, hypoxia, and malignant tumor have been previously studied by many and is expected to be effective in giving practical diagnostic support information. The information obtained by analyzing this spectral image has the advantage of visualizing and tracking the changes related with local events, in comparison with the surrounding conditions. Decades of multigroup studies have established the utility of spectral information as a research tool for obtaining information on gastrointestinal disease[24-26].

In addition to the method of measuring absorbance with a narrow-band wavelength filter, the method of evaluating the absorption spectrum in a wide wavelength range and the multivariate simultaneous analysis method were adopted to improve the accuracy of spectral analysis. These have been largely brought about by the contribution of not only endoscopic devices and spectroscopic devices but also the improvements in digitalization, transfer of data, and computer software that facilitate multivariate optimization calculation methods[27,28].

Spectral information in the biomedical field

Because the spectral information of the target substance is linked to the chemical information and its changes, it is possible to analyze the acquired spectral information and obtain the chemical information.

By applying a conventional spectral analysis method, spectral information on the chemical and histologic characteristics of the substances can be obtained[29-31]. Based on these analysis results, in the biomedical field, chemical and biological characterizations that are unique to the disease are expected to be recognized as new diagnostic support information. Specifically, capturing the effect of differences in the chemical structure between normal and diseased parts on the spectra may enable the utilization of a vast amount of information between the chemical structure and the spectra. In this respect, the chemical information and the medical diagnosis support information can be expected to be integrated and utilized[32-34].

As an example of capturing chemical structural changes as spectral information, **Figure 1** shows the changes in the spectral characteristics of oxyhemoglobin and deoxyhemoglobin secondary to the changes in the absorption of spectra, based on the difference in absorption spectrum between oxyhemoglobin and deoxyhemoglobin, according to oxygen binding.

The ratio of two substances calculated by quantitative spectral analysis is the SatO₂ information itself. This information is based on strong changes in hemoglobin in the wavelength range of 500-600 nm and the presence of detectable spectral absorption. The diffuse reflectance data of the colonic mucosa is also shown in **Figure 1**.

On the other hand, the physical structural changes can be detected by utilizing the fact that the nucleus is filled with a substance that has a higher refractive index, compared with that of the surrounding cytoplasm. By measuring the unique scattering pattern, the nuclear deformation of the cell can be estimated. Calculating the exact scattering behavior of a simple model system, such as a collection of spheres with specific size, density, and refractive index, and applying statistical processing may enable the diagnosis of the relationship between tissue changes secondary to nuclear variants and diseases. This information was reported to be used as support for the diagnosis of cancer[35-37]. In this study, the distribution of the size of the nucleus was estimated using the known properties of cell structure, such as the refractive index of the nucleus, and the measurements of periodic characterizations of the backscatter in

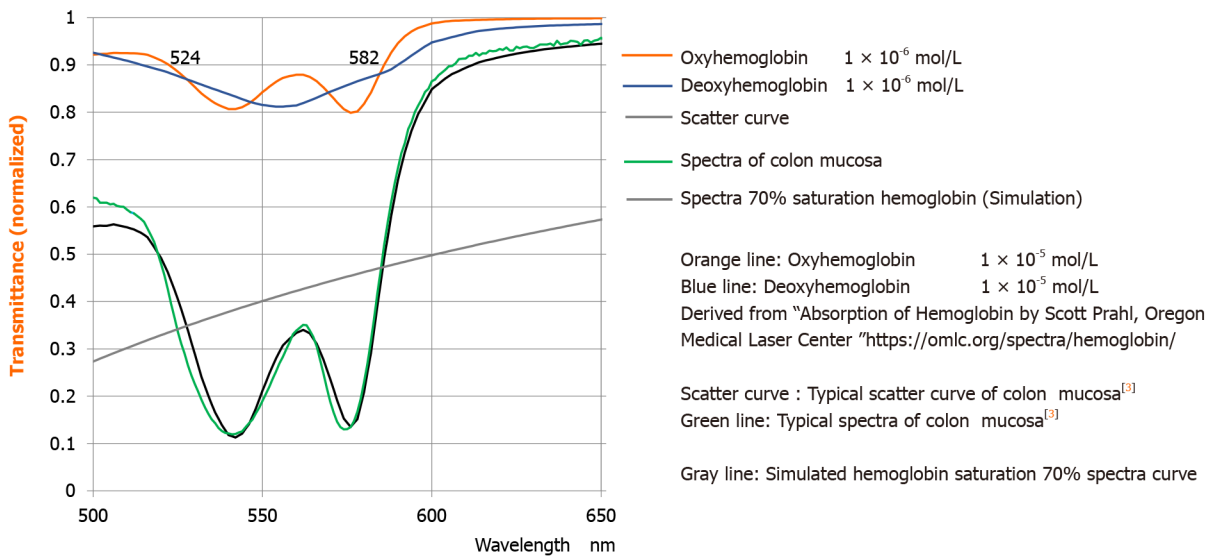


Figure 1 Spectra components oxyHb and deoxyHb and scatter.

the visible wavelength region. Analysis of nuclides has shown their effectiveness as a method for dysplasia assessment[38-40]. There have been many efforts to use DRS for disease detection and diagnosis. However, because of difficulties in data acquisition of back scatter (complicated optical system and higher light intensity is necessary) and the complex analysis in estimating nuclear size distribution, there have been few developments of practical commercial systems.

ANALYSIS OF SCATTERING INFORMATION

In the spectra information of human mucosa, scattering information dominates a large part of the information. Because of this reason, the explanation of spectral absorption and scattering is important for predicting the mucosa spectral information. Absorption and scattering comprise some of the optical processes that form the basis of the information obtained by DRS. Considering the effects of scattering on normal mucosa is basically an important issue. To estimate the concentration spectrochemically, the mathematical optimization described above is performed. The spectrum information of each component contained in this observed spectrum must be accurate. Several studies have focused on predicting light scattering spectra in the body to explain spectral information in the body.

The physical phenomenon is represented by the following equation, from which the relationship between scattering and transmittance can be derived (Formula 1)[5,41,42].

$$\mu_{scatter}(\lambda) = k_1 \left(\frac{\lambda}{\lambda_{max}} \right)^{(-k2)} + k_3 \left(\frac{\lambda}{\lambda_{max}} \right)^{(-4)}$$

In this absorption model for the mucosal surface, scatter is defined as the cumulative count of the components of the two types of scatter. The first and second terms on the right side of this expression are related to the Mie scatter and Rayleigh scatter, respectively. The parameters k1, k2, and k3 in this equation are calculated for the spectral simulation of scatter. λmax of 700 nm is employed as the wavelength area in our study.

Total scattering is divided into Rayleigh scattering and Mie scattering, and the influence of scattering on the diffuse reflectance measurement of the mucosa can be estimated by setting the parameters[43,44]. In our measurement experiment and in previous reports, the effectiveness of fitting using the abovementioned formula and measurement of the colonic mucosa and brain surface was confirmed to be greater with Mei scattering than with Rayleigh scattering[45].

The features of a disease in endoscopic imaging and spectral image analysis of the colon was examined and reported. Furthermore, a method of using spectral image information to monitor blood flow and SatO₂ during neurosurgery was proposed[46]. In the case of intestinal diseases, detection of various changes in the mucosal status on

the tissue surface can also be considered as changes in the spectrum secondary to diseases, such as ulcers, polyps, and inflammation[47]. For cases in which there can be changes in the optical path length or hemoglobin concentration secondary to ischemia, spectral information that considers these expected changes and the corresponding optical interpretation is required. Although many kinds of mucosa modeling were reported, there are few studies of modeling of the spectral information of unique disease, and detailed research results must be conducted for practical application[48-50].

DRS DATA ANALYSIS

In this report, a diffuse reflectance image of visible light was captured by illuminating the tissue of interest with a reference light and by quantitative analyses of spectral information of the reflected light from the tissue back to the detector. The reference light was a xenon light source with a wavelength of approximately 400-650 nm, which was the near-infrared range of ≥ 650 nm in endoscopy cases. Each 5 nm video graphics array (VGA) (640×480 pixels) took approximately 10 s to capture. Using a glass fiber-based fiberscope, the transmitted visible light image was captured with a spectral camera that was mentioned in the previous section[51]. The spectral information of stored data was quantitatively analyzed. An example of blood spectrum measurement is shown in Figure 1. In a typical colonic mucosa, the average hemoglobin SatO₂ was approximately 65%–80%.

This overlap can be exemplified by the measurement spectra of oxyhemoglobin (74%) and deoxyhemoglobin (26%) and scatter. The mathematical fitting to find this ratio was performed on all pixels to render a 2D SatO₂ display[52,53]. In the spectra analyses that used a large amount of spectral information for each 5-nm image, information other than the explanatory variables in the analysis was specified as an error; therefore, analysis of the spectral information of several pixels while maintaining the determined accuracy was possible. Additional factors, such as wavelength dependence of scattering, were minimized by a computerized process of providing a linear or polynomial correction term when fitting the spectrum (Formula 2)[54].

$$\begin{aligned} \mu(\lambda) &= -\log \frac{I_{\lambda}}{I_{0\lambda}} \\ &= \sum_j \varepsilon_j(\lambda) \cdot C_j \cdot d + offset \end{aligned}$$

Where (I/L) is the absorbance of wavelength λ , I_0 is reference intensity, I is observed intensity, j corresponds to the number of component, ε is the molar attenuation coefficient of the attenuating species at each wavelength (mol/L), C is the concentration of the attenuating species (mol/L), and d is the optical path of the component (L). In addition, the baseline offset was considered. The modified Beer-Lambert law was completed for each wavelength and each component.

This method of analysis was based on the Beer-Lambert law and was affected by the optical path length and the number of hemoglobin molecules[55]. In addition, it was necessary to compensate for the angle between the mucosal imaging area and the fiber incident surface angle. In this study, the information obtained by diffuse reflection was practically limited to the information near the surface layer of the mucosa. For example, using visible light, the standard signal was reported to be mainly secondary to hemoglobin absorption at a 0.25-mm surface tissue[56] and provided a good indicator of mucosa relative to the hemoglobin concentration and oxygenation[57].

This way, the average hemoglobin SatO₂ on the surface of the mucosa was accurately estimated by the DRS method. Because most blood in the measurement area was inside the mucosal capillaries, the tissue hemoglobin SatO₂ measured by DRS was estimated as the SatO₂ of hemoglobin in the mucosal capillaries. This made it possible to detect conditions of hypoxia caused by insufficient oxygen supply or excessive oxygen consumption of the mucosa.

In the actual measurement in the diseased part, blood concentration may have changed significantly because of bleeding. A high concentration of blood may be measured, especially in bleeding points. In this case, the spectra absorption was saturated, and the calculation of hemoglobin concentration and oxygenation became more difficult. In addition, despite attempts to create individual optical models, accurate diagnosis may not have been possible in special cases, such as in the presence of unexpected compounds; this limitation of this method must be recognized.

In other cases, such as the liver, which contains significant concentrations of cytochromes with a strong absorption spectrum in this range, measurement of hemoglobin oxygenation was not possible because of competing signals from other molecules. Regarding the irradiation of the reference light, generation of additional optical processes, such as fluorescence and Raman scattering, was considered. However, these kinds of light are usually weak and do not substantially affect the measurement.

METHOD OF SPECTRAL IMAGE CAPTURING

Hyperspectral image capturing and equipment

Basically, when detecting spectral information in a living body, comparison of the normal and diseased portions is necessary because of the limitations in reliability of the measurement results for each point, owing to biological individual difference. Using the capture technology of the 2D spectral information, the normal and diseased parts were effectively compared on the same screen. Moreover, sharing information with the output of the other imaging diagnostic equipment was possible. In this respect, 2D indication has been indispensable and extremely innovative in the field of diagnostic imaging support[58].

Because of limitations in the sensitivity region of the image sensor that is used for the detector, the spectroscopic device has been used in practice mainly with equipment that has a visible range of about 400-800 nm. Many studies have been conducted based on the observation that the spectral feature quantity changed in this wavelength region[59]. Spectral images have been recorded based on the functions of wavelength resolution with diffraction grating and light intensity measurement, using a photoelectric conversion element, i.e., charge coupled device and complementary metal oxide semiconductor (WAT-902H2 camera, Watec). This way, spectral image capturing using two typical capturing methods has been put to practical use.

The first method entailed optical image decomposition using a slit; the spectral information of one line of the slit was recorded in a 2D element. After recording the spectral information of each line, the recorded data were reconstructed as an image for each wavelength. This operation was repeated while moving the slits for vertical pixels to obtain 2D spectral information (Figure 2)[51,60].

For the second method, a switchable wavelength selection element was placed in front of a photoelectric conversion element. A typical case involved replacement of the conventional band-pass filter in front of the monochrome camera with a liquid crystal tunable filter (LCTF), repetition of high-speed switching of the transmission band, and image capturing in the wavelength range. Multiple filters limited the transmitted by combining the etalon plates. Furthermore, a liquid crystal material layer that had an anisotropic material of refractive index was placed in between the substrates of the etalon plates, and the optical path length of extraordinary light was controlled by applying a voltage. As a result, the transmission wavelength region was controlled[54, 61].

For example, when capturing a VGA 640 × 480-pixel spectral image, the spectral camera (Figure 2) captures one line in one image frame. Therefore, basically, the requirements were capturing an image in steps (usually pixels) toward the scan direction was necessary; 10 s, including 30 frames/s; and data transfer. Under this condition, the captured image will be distorted according to the movement of the object. However, because each line captured the entire wavelength range with a capture time of 1/30 sec, maintenance of the spectral information of pixels, which is the major feature of this method, was possible[51,60].

The second LCTF method was a method of arranging a LCTF in front of the image sensor, specifically a monochrome camera, and controlling the wavelength range incident on an image sensor (Figure 3). The time required for modulation was 50-80 ms for each image capture; this way, capturing a series of 400-800 nm for each of the 81 each 5-nm images, excluding data transfer, took around 5 s[54,61]. With this method, the screen capture for each transmission wavelength was realized; therefore, the motion on the image of the object being captured was recorded as a position change of the image in each wavelength, and this led to a calculation defect. As a solution to this problem, software for position compensation was used.

In both methods, the capture time depended on the operation speed of the light conversion element, the transfer speed of the captured data, and the processing speed of the time series information calculation. Therefore, equipment of higher performance, compared with that of commercially available equipment, was required

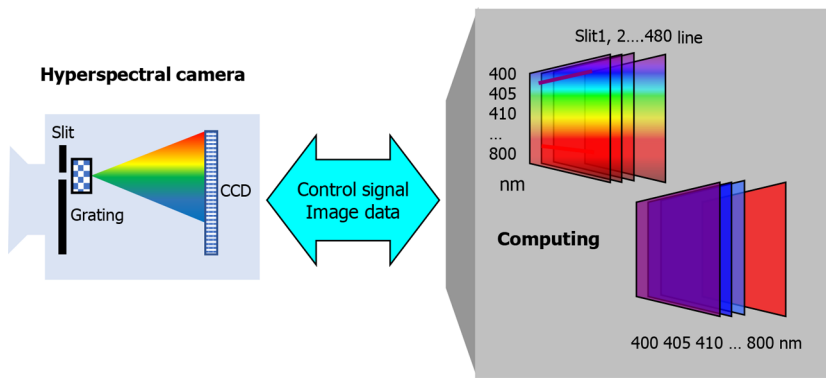


Figure 2 Scheme of hyperspectral camera.

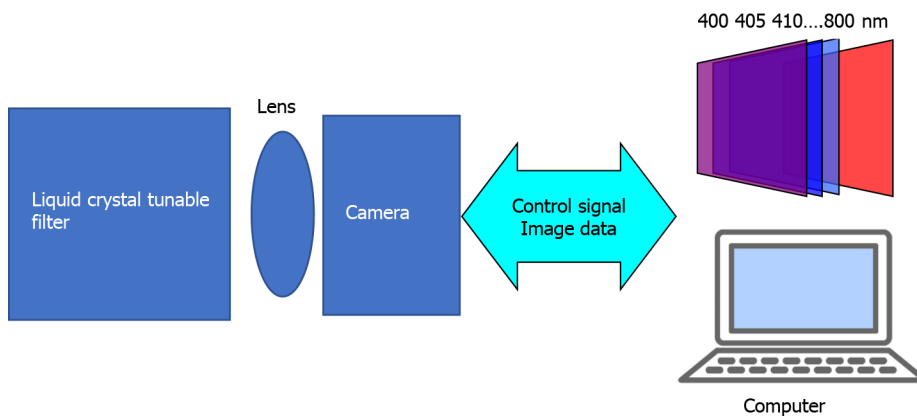


Figure 3 Scheme of liquid crystal tunable filter and digital camera combination.

for this information capture and processing.

PRACTICAL USE OF SPECTRAL ANALYSIS

As described above, spectral analysis acquires images by sampling wavelengths at equal intervals, and the movement of the apparatus itself or the movement or deformation of the object during capturing occurs; these make accurate spectral analysis extremely difficult. Although capturing many images is an unavoidable disadvantage, it may be solved by limiting the target spectral feature. And by short time capturing through reduction of the number of bands is to realized[5,48]. Multispectral method is unsuitable for tracking unknown chemicals and for characterizing chemical structure but is extremely effective for quantitative tracking of featured spectra changes.

By contrast, the spectral analysis is expected for the accurate detection and objective diagnosis of diseases. The effectiveness of spectral data in the medical field has been addressed in previous reports[46,49,50]. In addition, the application of blood flow and hemoglobin mapping for implantation surgery using a small animal model was proposed[62,63].

Multispectral endoscope system is used to indicate r-Hconc and saturation generated with 2D display, which is analyzed using the spectral feature of the three multispectral images. This method achieved an image output of 7.5 frames/s was reported. The system enables to indicate hemoglobin saturation (SatO₂) of the mucosa with a practical frame rate for normal examination (Figure 4).

Diffuse reflection spectroscopy for gastrointestinal examination is expectedly applied in various ways for the noninvasive diagnosis of diseases[64,65].

The proposed technique for the detection of hypoxic areas is based on Hb-oxygen dynamics, and detailed observation of the gastrointestinal mucosa is important for endoscopic detection and diagnosis. Previous studies reported a successful spectroscopic analysis of the gastrointestinal mucosa, with some characterizing both normal

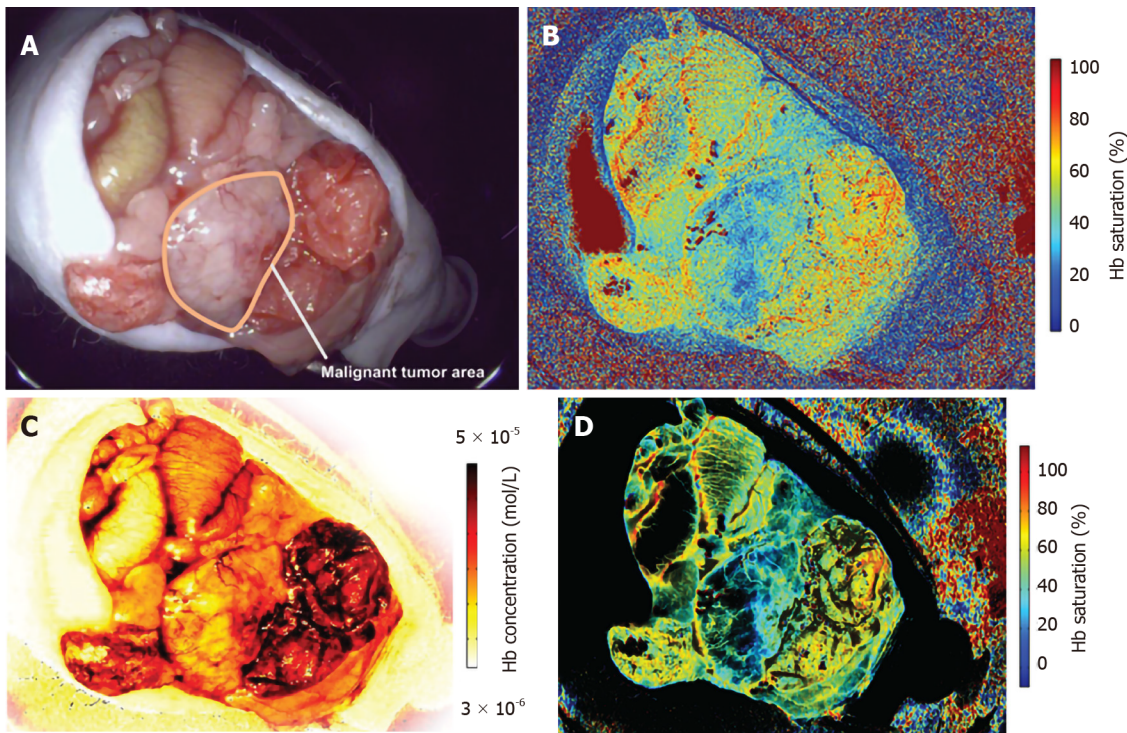


Figure 4 The system enables to indicate hemoglobin saturation of the mucosa with a practical frame rate for normal examination. An area with relatively high Hb concentration area is enhanced by an Hb concentration mask. The higher Hb concentration and lower Hb saturation areas that are influenced by the tumor are observed as a blue area. A: Experimental cancer model. Red–green–blue video endoscope image of the mouse viscera. The tumor area is outlined by a white line; B: Hb saturation map of the tumor generated by the endoscope system; C: Hb concentration map of the tumor generated by the endoscope system; D: Hb concentration-masked Hb saturation map.

and abnormal tissues[66,67].

With regard to the spectral data of the colonic mucosa, marked characteristics in relative Hb concentration and blood oxygenation have been reported to be also detected for the tumor. Differences in the relative Hb concentration and saturation between malignant tumors and non-malignant mucosa have been previously investigated and reported as a “high Hb concentration level and lower Hb saturation for malignant tumors.” To compare actual individual differences between Hb concentration and normal tissue saturation, superiority of the “spatial indication,” including diseased and normal tissue, has been confirmed[7,68-70].

The logical combination of the relative Hb concentration and saturation will also be useful to detect notable regions.

DISCUSSION

Several studies have reported the effect of scattered spectral data on human mucosa[6, 19]. In this study and previous studies, the components of diffuse reflectance data of normal intestinal mucosa were explained mainly by oxyhemoglobin, deoxyhemoglobin, and scattering; detection of differences between normal and diseased parts as an abnormal ratio of these three components is expected. As shown above, the use of multispectral analysis reduced the device load of wavelength shift capturing and transfer and allowed near real-time monitoring of r-Hconc and saturation. In this study, the fusion of information on r-Hconc and SatO₂ enabled the extraction of partial data on high blood flow with high SatO₂ and high blood flow with low oxygen. This fusion information is expected to support the diagnosis and identification of inflammation and malignant tumors.

Endoscope system, which enables the indication of 2D SatO₂ and r-Hconc mapping, was developed. Display and recording of blood concentration and mucosal SatO₂ changes over time were possible with the video rate. The system paved the way to SatO₂ evaluation for general endoscopic examination. Moreover, an animal study has shown that reduced SatO₂ in tissues following vascular occlusion in a controlled setting, including arterial and venous occlusion models, is reproducible. These results

Table 1 Application of indicating relative hemoglobin concentration and saturation function to surgical operation

Department	Target disease	Expected results
Neurosurgery	(1) Brain tumor; and (2) Cerebral infarction: Detection of diseased area	(1) Improvement of postoperative outcome in terms of oncologic and functional preservation; and (2) Diagnostic improvement
Urology	Partial nephrectomy of renal tumor: Detection of area of ischemia secondary to occlusion of a dominant artery	Improvement of postoperative outcome in terms of oncologic and functional preservation
Gynecology	Trachelectomy for cervical cancer: Assessment of relativity between blood flow and fertility after anastomosis	Decision on the optimal reconstruction method
Gastroenterology surgery	Organ resection for gastrointestinal cancer: Assessment of the organ after resection and reconstruction. Strangulation ileus and hernia: Conformation of organ and tissue viability-related blood flow and oxygen saturation	Reduction of postoperative complications by assessment of real-time organ viability
Plastic surgery	Skin transplantation, including breast reconstruction: Confirmation of transplanted organ and tissue viability-related blood flow and oxygen saturation. Keloid scar: Relative assessment of keloid scar formation-related blood flow and oxygen saturation	(1) Improvement of reconstructive surgery; and (2) Establishment of knowledge on the oxygen saturation of wound tissue for prevention of keloid formation
Ocular	Diabetic retinopathy: Evaluation of the oxygen saturation of fundus blood vessels	Establishment of evaluation and treatment for diabetic retinopathy

were consistent with decreased SatO₂ in the mucosa when blood flow is blocked after arterial occlusion and with increased SatO₂ during blood flow restoration. Moreover, these results led to the evaluation of biological activities.

Application of reflectance spectroscopy

DRS endoscopy is expected to be used as a tool to investigate the roles of mucosal perfusion and hemoglobin oxygenation in the pathophysiology of various diseases, such as peptic ulcer disease, inflammatory bowel disease, and portal hypertensive gastritis. Other studies have investigated the effects of various vasoactive agents on mucosal perfusion and physiologic interventions, such as brain tumor[2,71,72]. Moreover, research on the application of reflectance spectrophotometry on ulcer disease has been reported[73]. In animal models, studies reported decreased hemoglobin concentration and SatO₂ after ligation of arterioles that fed the mucosa. Another research noted that unlike pulse oximetry, the diffuse reflectance method provided reliable measurements in areas other than the aorta. This recent study convincingly demonstrated the application of the diffuse reflectance technique to continuous monitoring of mucosal perfusion and oxygenation in the emergency setting[73].

Reflectance spectroscopy as a future technology

A decade ago, spectral analysis started with an old spectroscopic system. Nowadays, real-time display of diagnostic assistance information is possible by acquisition and analysis of data, based on 2D spectral information. Spectral imaging, which has been researched in recent years, has opened the way to the acquisition and analysis of 2D spectral information, as well as fusion with new diagnostic support information based on chemical and biological knowledge. However, improvement of device performance as a practical equipment is essential.

Although a multispectral image provides limited information, it provides a device that can display data with realistic accuracy and speed within the scope of currently available technology based on rapid measurement and analysis. The technology introduced in this report included an example of controlling the light source of an endoscopic system, but the development of a multispectral camera was already considered. The system, which is equipped with the function of capturing multispectral information and displaying diagnostic support information, will be able to expand its field of application. For example, the system is expected to provide important monitoring information for evaluating oxygen delivery to selected tissues, such as the esophagus, stomach, and rectal mucosa. Moreover, the actively available areas of this technique for local hemoglobin concentration and oxygenation have also been applied in the field of surgical and radiologic vascular assessment. The table below shows the expected fields that would use blood concentration and SatO₂ display in the surgical field. Multiple trials are currently seeking practical applications (Table 1).

CONCLUSION

Research on the analysis of spectral information of the human gastrointestinal mucosa was advanced, and hemoglobin concentration and SatO₂ changes were detected in blood, the main spectral component in the visible region. A practical endoscopic system was reported to allow real-time quantitative 2D display of hemoglobin concentration and SatO₂ of human gastrointestinal mucosa, indicating information for the detection and diagnosis of diseased areas.

ACKNOWLEDGEMENTS

The author expresses his gratitude in pre-agreement with all the colleagues above. The comments provided by corresponding author and reviewers have greatly improved the clarity of the manuscript.

REFERENCES

- 1 **Teng Y**, Ding H, Gong Q, Jia Z, Huang L. Monitoring cerebral oxygen saturation during cardiopulmonary bypass using near-infrared spectroscopy: the relationships with body temperature and perfusion rate. *J Biomed Opt* 2006; **11**: 024016 [PMID: 16674206 DOI: 10.1117/1.2187422]
- 2 **Orihashi K**, Sueda T, Okada K, Imai K. Near-infrared spectroscopy for monitoring cerebral ischemia during selective cerebral perfusion. *Eur J Cardiothorac Surg* 2004; **26**: 907-911 [PMID: 15519181 DOI: 10.1016/j.ejcts.2004.06.014]
- 3 **Kumashiro R**, Konishi K, Chiba T, Akahoshi T, Nakamura S, Murata M, Tomikawa M, Matsumoto T, Maehara Y, Hashizume M. Integrated Endoscopic System Based on Optical Imaging and Hyperspectral Data Analysis for Colorectal Cancer Detection. *Anticancer Res* 2016; **36**: 3925-3932 [PMID: 27466495]
- 4 **Utzinger U**, Brewer M, Silva E, Gershenson D, Blast RC Jr, Follen M, Richards-Kortum R. Reflectance spectroscopy for in vivo characterization of ovarian tissue. *Lasers Surg Med* 2001; **28**: 56-66 [PMID: 11430444 DOI: 10.1002/1096-9101(2001)28:1<56::AID-LSM1017>3.0.CO;2-L]
- 5 **Wirkert SJ**, Clancy NT, Stoyanov D, Arya S, Hanna GB, Schlemmer HP, Sauer P, Elson DS, Maier-Hein L. Endoscopic Sheffield index for unsupervised in vivo spectral band selection. In: International Workshop on Computer-Assisted and Robotic Endoscopy. Springer, Cham, 2014: 110-120
- 6 **Zonios G**, Perelman LT, Backman V, Manoharan R, Fitzmaurice M, Van Dam J, Feld MS. Diffuse reflectance spectroscopy of human adenomatous colon polyps in vivo. *Appl Opt* 1999; **38**: 6628-6637 [PMID: 18324198 DOI: 10.1364/ao.38.006628]
- 7 **Bard MP**, Amelink A, Hegt VN, Graveland WJ, Sterenborg HJ, Hoogsteden HC, Aerts JG. Measurement of hypoxia-related parameters in bronchial mucosa by use of optical spectroscopy. *Am J Respir Crit Care Med* 2005; **171**: 1178-1184 [PMID: 15709054 DOI: 10.1164/rccm.200501-046OC]
- 8 **Subhash N**, Mallia JR, Thomas SS, Mathews A, Sebastian P, Madhavan J. Oral cancer detection using diffuse reflectance spectral ratio R540/R575 of oxygenated hemoglobin bands. *J Biomed Opt* 2006; **11**: 014018 [PMID: 16526895 DOI: 10.1117/1.2165184]
- 9 **Zonios GI**. Diffuse reflectance spectroscopy of human colon tissue 1998. MIT 1998
- 10 **Stelzle F**, Tangermann-Gerk K, Adler W, Zam A, Schmidt M, Douplik A, Nkenke E. Diffuse reflectance spectroscopy for optical soft tissue differentiation as remote feedback control for tissue-specific laser surgery. *Lasers Surg Med* 2010; **42**: 319-325 [PMID: 20432281 DOI: 10.1002/lsm.20909]
- 11 **Chance B**. Rapid and sensitive spectrophotometry. I. The accelerated and stopped-flow methods for the measurement of the reaction kinetics and spectra of unstable compounds in the visible region of the spectrum. *Rev Sci Instrum* 1951; **22**: 619-627 [DOI: 10.1063/1.1746019]
- 12 **Chance B**, Mayevsky A, Goodwin C, Mela L. Factors in oxygen delivery to tissue. *Microvasc Res* 1974; **8**: 276-282 [PMID: 4155043 DOI: 10.1016/s0026-2862(74)80003-8]
- 13 **Mohri T**, Mohri C, Yamadori F. Tubaloscope: flexible glassfiber endoscope for intratubal observation. *Endoscopy* 1970; **2**: 226-230 [DOI: 10.1055/s-0028-1098472]
- 14 **Leung FW**, Slodownik E, Jensen DM, Van Deventer GM, Guth PH. Gastroduodenal mucosal hemodynamics by endoscopic reflectance spectrophotometry. *Gastrointest Endosc* 1987; **33**: 284-288 [PMID: 3653647 DOI: 10.1016/s0016-5107(87)71599-5]
- 15 **Sato N**, Kawano S, Kamada T, Takeda M. Hemodynamics of the gastric mucosa and gastric ulceration in rats and in patients with gastric ulcer. *Dig Dis Sci* 1986; **31**: 35S-41S [PMID: 3943456 DOI: 10.1007/BF01309321]
- 16 **Harris ND**, Ibrahim S, Radatz M, Ward JD. Measurements of oxygen saturation in normal human sural nerve by micro-lightguide spectrophotometry and endoscopy. *Adv Exp Med Biol* 1997; **428**: 15-20 [PMID: 9500023 DOI: 10.1007/978-1-4615-5399-1_3]

- 17 **Kuzin NM**, Loschenov VB, Stratonnikov AA, Artemjeva OV, Levkin VV, Kharnas SS. Method of oxygenation saturation evaluation of stomach mucous after subtotal cancer resection. *Proceedings of the SPIE*, 1994; 98-101
- 18 **Bigio IJ**, Mourant JR, Boyer JD, Johnson TM, Shimada T, Conn RL. Noninvasive identification of bladder cancer with subsurface backscattered light. In: *Advances in Laser and Light Spectroscopy to Diagnose Cancer and Other Diseases*; International Society for Optics and Photonics. *Proceedings of the SPIE*, 1994; 26-35
- 19 **Friebel M**, Helfmann J, Netz U, Meinke M. Influence of oxygen saturation on the optical scattering properties of human red blood cells in the spectral range 250 to 2,000 nm. *J Biomed Opt* 2009; **14**: 034001 [PMID: [19566295](#) DOI: [10.1117/1.3127200](#)]
- 20 **Friedland S**, Benaron D, Parachikov I, Soetikno R. Measurement of mucosal capillary hemoglobin oxygen saturation in the colon by reflectance spectrophotometry. *Gastrointest Endosc* 2003; **57**: 492-497 [PMID: [12665758](#) DOI: [10.1067/mge.2003.162](#)]
- 21 **Claridge E**, Hidović-Rowe D, Taniere P, Ismail T. Quantifying mucosal blood volume fraction from multispectral images of the colon. In: *Medical Imaging 2007: Physiology, Function, and Structure from Medical Images*; International Society for Optics and Photonics. *Proceedings of the SPIE*, 2007: 65110C
- 22 **Kamat V**. Pulse oximetry. *Indian J Anaesth* 2002; **46**: 261-268
- 23 **Bagha S**, Shaw L. A real time analysis of PPG signal for measurement of SpO₂ and pulse rate. *Int J Comput Appl* 2011; **36**: 45-50
- 24 **Leung FW**. Endoscopic reflectance spectrophotometry and visible light spectroscopy in clinical gastrointestinal studies. *Dig Dis Sci* 2008; **53**: 1669-1677 [PMID: [17932761](#) DOI: [10.1007/s10620-007-0026-8](#)]
- 25 **Bashkatov AN**, Genina EA, Kochubey VI, Gavrilova AA, Kapralov SV, Grishaev VA, Tuchin VV. Optical properties of human stomach mucosa in the spectral range from 400 to 2000 nm: prognosis for gastroenterology. *Med Laser Appl* 2007; **22**: 95-104 [DOI: [10.1016/j.mla.2007.07.003](#)]
- 26 **Van Noord D**, Sana A, Benaron DA, Pattynama PM, Verhagen HJ, Hansen BE, Kuipers EJ, Mensink PB. Endoscopic visible light spectroscopy: a new, minimally invasive technique to diagnose chronic GI ischemia. *Gastrointest Endosc* 2011; **73**: 291-298 [PMID: [21168842](#) DOI: [10.1016/j.gie.2010.10.025](#)]
- 27 **Thanasoulis NC**, Parisis NA, Evmiridis NP. Multivariate chemometrics for the forensic discrimination of blue ball-point pen inks based on their Vis spectra. *Forensic Sci Int* 2003; **138**: 75-84 [PMID: [14642722](#) DOI: [10.1016/j.forsciint.2003.08.014](#)]
- 28 **Noda I**. Generalized two-dimensional correlation method applicable to infrared, Raman, and other types of spectroscopy. *Appl Spectrosc* 1993; **47**: 1329-1336 [DOI: [10.1366/0003702934067694](#)]
- 29 **Rossel RV**, Walvoort DJJ, McBratney AB, Janik LJ, Skjemstad JO. Visible, near infrared, mid infrared or combined diffuse reflectance spectroscopy for simultaneous assessment of various soil properties. *Geoderma* 2006; **131**: 59-75
- 30 **Tsumura N**, Kawabuchi M, Haneishi H, Miyake Y. Mapping pigmentation in human skin from a multi-channel visible spectrum image by inverse optical scattering technique. *J Imag Sci Technol* 2001; **45**: 444-450
- 31 **Zijlstra WG**, Buursma A, van Assendelft OW. Visible and near infrared absorption spectra of human and animal haemoglobin: determination and application. CRC Press: Utrecht; Boston VSP, 2000
- 32 **Bigio IJ**, Bown SG, Briggs G, Kelley C, Lakhani S, Pickard D, Ripley PM, Rose IG, Saunders C. Diagnosis of breast cancer using elastic-scattering spectroscopy: preliminary clinical results. *J Biomed Opt* 2000; **5**: 221-228 [PMID: [10938787](#) DOI: [10.1117/1.429990](#)]
- 33 **Zhu C**, Palmer GM, Breslin TM, Harter J, Ramanujam N. Diagnosis of breast cancer using diffuse reflectance spectroscopy: Comparison of a Monte Carlo versus partial least squares analysis based feature extraction technique. *Lasers Surg Med* 2006; **38**: 714-724 [PMID: [16799981](#) DOI: [10.1002/Lsm.20356](#)]
- 34 **Horecker BL**. The absorption spectra of hemoglobin and its derivatives in the visible and near infrared regions. *J Biol Chem* 1943; **148**: 173-183 [DOI: [10.1016/S0021-9258\(18\)72329-6](#)]
- 35 **Siegel MP**, Kim YL, Roy HK, Wali RK, Backman V. Assessment of blood supply in superficial tissue by polarization-gated elastic light-scattering spectroscopy. *Appl Opt* 2006; **45**: 335-342 [PMID: [16422163](#) DOI: [10.1364/ao.45.000335](#)]
- 36 **Roy HK**, Kim YL, Liu Y, Wali RK, Goldberg MJ, Turzhitsky V, Horwitz J, Backman V. Risk stratification of colon carcinogenesis through enhanced backscattering spectroscopy analysis of the uninvolved colonic mucosa. *Clin Cancer Res* 2006; **12**: 961-968 [PMID: [16467111](#) DOI: [10.1158/1078-0432.CCR-05-1605](#)]
- 37 **Perelman LT**, Backman V, Wallace M, Zonios G, Manoharan R, Nusrat A, Shields S, Seiler M, Lima T, Hamano T, Itzkan I, Van Dam J, Crawford JM, Feld MS. Observation of periodic fine structure in reflectance from biological tissue: a new technique for measuring nuclear size distribution. *Phys Rev Lett* 1998; **80**: 627 [DOI: [10.1103/PhysRevLett.80.627](#)]
- 38 **Backman V**, Gurjar R, Badizadegan K, Itzkan I, Dasari RR, Perelman LT, Feld MS. Polarized light scattering spectroscopy for quantitative measurement of epithelial cellular structures in situ. *IEEE J Select Topics Quantum Electron* 1999; **5**: 1019-1026 [DOI: [10.1109/2944.796325](#)]
- 39 **Sokolov K**, Drezek R, Gossage K, Richards-Kortum R. Reflectance spectroscopy with polarized light: is it sensitive to cellular and nuclear morphology. *Opt Express* 1999; **5**: 302-317 [PMID: [16467111](#) DOI: [10.1158/1078-0432.CCR-05-1605](#)]

- 19401735 DOI: [10.1364/oe.5.000302](https://doi.org/10.1364/oe.5.000302)]
- 40 **Sokolov K**, Follen M, Richards-Kortum R. Optical spectroscopy for detection of neoplasia. *Curr Opin Chem Biol* 2002; **6**: 651-658 [PMID: [12413550](https://pubmed.ncbi.nlm.nih.gov/12413550/) DOI: [10.1016/s1367-5931\(02\)00381-2](https://doi.org/10.1016/s1367-5931(02)00381-2)]
 - 41 **Hidović-Rowe D**, Claridge E. Modelling and validation of spectral reflectance for the colon. *Phys Med Biol* 2005; **50**: 1071-1093 [PMID: [15798309](https://pubmed.ncbi.nlm.nih.gov/15798309/) DOI: [10.1088/0031-9155/50/6/003](https://doi.org/10.1088/0031-9155/50/6/003)]
 - 42 **Saager RB**, Truong A, Cuccia DJ, Durkin AJ. Method for depth-resolved quantitation of optical properties in layered media using spatially modulated quantitative spectroscopy. *J Biomed Opt* 2011; **16**: 077002 [PMID: [21806282](https://pubmed.ncbi.nlm.nih.gov/21806282/) DOI: [10.1117/1.3597621](https://doi.org/10.1117/1.3597621)]
 - 43 **Saidi IS**, Jacques SL, Tittel FK. Mie and Rayleigh modeling of visible-light scattering in neonatal skin. *Appl Opt* 1995; **34**: 7410-7418 [PMID: [21060615](https://pubmed.ncbi.nlm.nih.gov/21060615/) DOI: [10.1364/AO.34.007410](https://doi.org/10.1364/AO.34.007410)]
 - 44 **Mirkovic J**, Lau C, McGee S, Yu CC, Nazemi J, Galindo L, Feng V, Darragh T, de Las Morenas A, Crum C, Stier E, Feld M, Badizadegan K. Effect of anatomy on spectroscopic detection of cervical dysplasia. *J Biomed Opt* 2009; **14**: 044021 [PMID: [19725732](https://pubmed.ncbi.nlm.nih.gov/19725732/) DOI: [10.1117/1.3194142](https://doi.org/10.1117/1.3194142)]
 - 45 **Yudovsky D**, Pilon L. Rapid and accurate estimation of blood saturation, melanin content, and epidermis thickness from spectral diffuse reflectance. *Appl Opt* 2010; **49**: 1707-1719 [PMID: [20357850](https://pubmed.ncbi.nlm.nih.gov/20357850/) DOI: [10.1364/AO.49.001707](https://doi.org/10.1364/AO.49.001707)]
 - 46 **Mori M**, Chiba T, Nakamizo A, Kumashiro R, Murata M, Akahoshi T, Tomikawa M, Kikkawa Y, Yoshimoto K, Mizoguchi M, Sasaki T, Hashizume M. Intraoperative visualization of cerebral oxygenation using hyperspectral image data: a two-dimensional mapping method. *Int J Comput Assist Radiol Surg* 2014; **9**: 1059-1072 [PMID: [24737109](https://pubmed.ncbi.nlm.nih.gov/24737109/) DOI: [10.1007/s11548-014-0989-9](https://doi.org/10.1007/s11548-014-0989-9)]
 - 47 **Mirabal YN**, Chang SK, Atkinson EN, Malpica A, Follen M, Richards-Kortum R. Reflectance spectroscopy for in vivo detection of cervical precancer. *J Biomed Opt* 2002; **7**: 587-594 [PMID: [12421125](https://pubmed.ncbi.nlm.nih.gov/12421125/) DOI: [10.1117/1.1502675](https://doi.org/10.1117/1.1502675)]
 - 48 **Chiba T**, Obara Y, Murata M, Akahoshi T. Advanced multispectral image-processing endoscopy system for visualizing two-dimensional hemoglobin saturation and relative hemoglobin concentration. *Endosc Int Open* 2019; **7**: E1442-E1447 [PMID: [31673616](https://pubmed.ncbi.nlm.nih.gov/31673616/) DOI: [10.1055/a-0990-9189](https://doi.org/10.1055/a-0990-9189)]
 - 49 **Liu Z**, Wang H, Li Q. Tongue tumor detection in medical hyperspectral images. *Sensors (Basel)* 2012; **12**: 162-174 [PMID: [22368462](https://pubmed.ncbi.nlm.nih.gov/22368462/) DOI: [10.3390/s120100162](https://doi.org/10.3390/s120100162)]
 - 50 **Nallala J**, Jeynes C, Saunders S, Smart N, Lloyd G, Riley L, Salmon D, Stone N. Characterization of colorectal mucus using infrared spectroscopy: a potential target for bowel cancer screening and diagnosis. *Lab Invest* 2020; **100**: 1102-1110 [PMID: [32203151](https://pubmed.ncbi.nlm.nih.gov/32203151/) DOI: [10.1038/s41374-020-0418-3](https://doi.org/10.1038/s41374-020-0418-3)]
 - 51 **Satori S**, Aoyanagi Y, Hara U, Mitsuhashi R, Takeuchi Y. Hyperspectral sensor HSC3000 for nano-satellite TAIKI. In: Multispectral, hyperspectral, and ultraspectral remote sensing technology, techniques, and applications II; International Society for Optics and Photonics. Proceedings of the SPIE, 2008: 71490M
 - 52 **Champagne CM**, Staenz K, Bannari A, McNairn H, Deguise JC. Validation of a hyperspectral curve-fitting model for the estimation of plant water content of agricultural canopies. *Remote Sens Environ* 2003; **87**: 148-160 [DOI: [10.1016/S0034-4257\(03\)00137-8](https://doi.org/10.1016/S0034-4257(03)00137-8)]
 - 53 **Brown AJ**. Spectral curve fitting for automatic hyperspectral data analysis. *IEEE Trans Geosci Remote Sensing* 2006; **44**: 1601-1608 [DOI: [10.1109/TGRS.2006.870435](https://doi.org/10.1109/TGRS.2006.870435)]
 - 54 **Aharon O**, Abdulhalim I. Liquid crystal Lyot tunable filter with extended free spectral range. *Opt Express* 2009; **17**: 11426-11433 [PMID: [19582057](https://pubmed.ncbi.nlm.nih.gov/19582057/) DOI: [10.1364/oe.17.011426](https://doi.org/10.1364/oe.17.011426)]
 - 55 **Shimada M**, Masuda Y, Yamada Y, Itoh M, Takahashi M, Yatagai T. Explanation of human skin color by multiple linear regression analysis based on the modified Lambert-Beer law. *Opt Rev* 2000; **7**: 348-352 [DOI: [10.1007/s10043-000-0348-7](https://doi.org/10.1007/s10043-000-0348-7)]
 - 56 **Temmesfeld-Wollbrück B**, Szalay A, Mayer K, Olschewski H, Seeger W, Grimminger F. Abnormalities of gastric mucosal oxygenation in septic shock: partial responsiveness to doxepamine. *Am J Respir Crit Care Med* 1998; **157**: 1586-1592 [PMID: [9603142](https://pubmed.ncbi.nlm.nih.gov/9603142/) DOI: [10.1164/ajrccm.157.5.9710017](https://doi.org/10.1164/ajrccm.157.5.9710017)]
 - 57 **Panés J**, Bordas JM, Piqué JM, Bosch J, García-Pagán JC, Feu F, Casadevall M, Terés J, Rodés J. Increased gastric mucosal perfusion in cirrhotic patients with portal hypertensive gastropathy. *Gastroenterology* 1992; **103**: 1875-1882 [PMID: [1451980](https://pubmed.ncbi.nlm.nih.gov/1451980/) DOI: [10.1016/0016-5085\(92\)91447-c](https://doi.org/10.1016/0016-5085(92)91447-c)]
 - 58 **Manolakis D**, Marden D, Shaw GA. Hyperspectral image processing for automatic target detection applications. *Lincoln Lab J* 2003; **14**: 79-116
 - 59 **Richard C**, Courcier T, Pittet P, Martel S, Ouellet L, Lu GN, Aimez V, Charette PG. CMOS buried quad p-n junction photodetector for multi-wavelength analysis. *Opt Express* 2012; **20**: 2053-2061 [PMID: [22330446](https://pubmed.ncbi.nlm.nih.gov/22330446/) DOI: [10.1364/OE.20.002053](https://doi.org/10.1364/OE.20.002053)]
 - 60 **Shapey J**, Xie Y, Nabavi E, Bradford R, Saeed SR, Ourselin S, Vercauteren T. Intraoperative multispectral and hyperspectral label-free imaging: A systematic review of in vivo clinical studies. *J Biophotonics* 2019; **12**: e201800455 [PMID: [30859757](https://pubmed.ncbi.nlm.nih.gov/30859757/) DOI: [10.1002/jbio.201800455](https://doi.org/10.1002/jbio.201800455)]
 - 61 **Lee H**, Kim MH. Building a two-way hyperspectral imaging system with liquid crystal tunable filters. In: International Conference on Image and Signal Processing. Springer, Cham, 2014: 26-34
 - 62 **Sorg BS**, Moeller BJ, Donovan O, Cao Y, Dewhirst MW. Hyperspectral imaging of hemoglobin saturation in tumor microvasculature and tumor hypoxia development. *J Biomed Opt* 2005; **10**: 44004 [PMID: [16178638](https://pubmed.ncbi.nlm.nih.gov/16178638/) DOI: [10.1117/1.2003369](https://doi.org/10.1117/1.2003369)]
 - 63 **Biel NM**, Lee JA, Sorg BS, Siemann DW. Limitations of the dorsal skinfold window chamber model in evaluating anti-angiogenic therapy during early phase of angiogenesis. *Vasc Cell* 2014; **6**: 17 [PMID: [25101168](https://pubmed.ncbi.nlm.nih.gov/25101168/) DOI: [10.1186/2045-824X-6-17](https://doi.org/10.1186/2045-824X-6-17)]

- 64 **Ortega S**, Fabelo H, Iakovidis DK, Koulaouzidis A, Callico GM. Use of Hyperspectral/Multispectral Imaging in Gastroenterology. Shedding Some-Different-Light into the Dark. *J Clin Med* 2019; **8** [PMID: 30609685 DOI: 10.3390/jcm8010036]
- 65 **Gu X**, Han Z, Yao L, Zhong Y, Shi Q, Fu Y, Liu C, Wang X, Xie T. Image enhancement based on in vivo hyperspectral gastroscopic images: a case study. *J Biomed Opt* 2016; **21**: 101412 [PMID: 27206742 DOI: 10.1117/1.JBO.21.10.101412]
- 66 **Kaneko K**, Yamaguchi H, Saito T, Yano T, Oono Y, Ikematsu H, Nomura S, Sato A, Kojima M, Esumi H, Ochiai A. Hypoxia imaging endoscopy equipped with laser light source from preclinical live animal study to first-in-human subject research. *PLoS One* 2014; **9**: e99055 [PMID: 24915532 DOI: 10.1371/journal.pone.0099055]
- 67 **Yoon J**, Joseph J, Waterhouse DJ, Luthman AS, Gordon GSD, di Pietro M, Januszewicz W, Fitzgerald RC, Bohndiek SE. A clinically translatable hyperspectral endoscopy (HySE) system for imaging the gastrointestinal tract. *Nat Commun* 2019; **10**: 1902 [PMID: 31015458 DOI: 10.1038/s41467-019-09484-4]
- 68 **Wang HW**, Jiang JK, Lin CH, Lin JK, Huang GJ, Yu JS. Diffuse reflectance spectroscopy detects increased hemoglobin concentration and decreased oxygenation during colon carcinogenesis from normal to malignant tumors. *Opt Express* 2009; **17**: 2805-2817 [PMID: 19219185 DOI: 10.1364/oe.17.002805]
- 69 **Maxim PG**, Carson JJ, Benaron DA, Loo BW Jr, Xing L, Boyer AL, Friedland S. Optical detection of tumors in vivo by visible light tissue oximetry. *Technol Cancer Res Treat* 2005; **4**: 227-234 [PMID: 15896077 DOI: 10.1177/153303460500400301]
- 70 **Hidović-Rowe D**, Claridge E, Ismail T, Taniere P, Graham J. Analysis of multispectral images of the colon to reveal histological changes characteristic of cancer. *Med Image Underst Anal MIUA* 2006; **1**: 66-70
- 71 **Nouri D**, Lucas Y, Treuillet S. Calibration and test of a hyperspectral imaging prototype for intra-operative surgical assistance. In: Medical Imaging 2013: Digital Pathology; International Society for Optics and Photonics. Proceedings of the SPIE, 2013: 86760P
- 72 **Gebhart SC**, Thompson RC, Mahadevan-Jansen A. Liquid-crystal tunable filter spectral imaging for brain tumor demarcation. *Appl Opt* 2007; **46**: 1896-1910 [PMID: 17356636 DOI: 10.1364/ao.46.001896]
- 73 **Jeffcoate WJ**, Clark DJ, Savic N, Rodmell PI, Hinchliffe RJ, Musgrove A, Game FL. Use of HSI to measure oxygen saturation in the lower limb and its correlation with healing of foot ulcers in diabetes. *Diabet Med* 2015; **32**: 798-802 [PMID: 25864911 DOI: 10.1111/dme.12778]



Published by **Baishideng Publishing Group Inc**
7041 Koll Center Parkway, Suite 160, Pleasanton, CA 94566, USA

Telephone: +1-925-3991568

E-mail: bpgoffice@wjgnet.com

Help Desk: <https://www.f6publishing.com/helpdesk>

<https://www.wjgnet.com>

